INVESTIGATION OF COASTAL WIND FIELDS OVER THE BLACK SEA USING ENVISAT SYNTHETIC APERTURE RADAR IMAGES

Werner Alpers [(1)], ***Andrei Yu. Ivanov*** [(2)], ***Knut-Frode Dagestad*** [(3)]

[(1)] *Centre for Marine and Atmospheric Sciences (ZMAW), Institute of Oceanography, University of Hamburg, Bundesstrasse 53, 20146 Hamburg, Germany, Email: werner.alpers@zmaw.de*

[(2)] *P.P. Shirshov Institute of Oceanology, Russian Academy of Sciences, Moscow, Nakhimovsky prospect 36, Moscow, 117997, Russia, Email: ivanoff@ocean.ru*

[(3)] *Nansen Environmental and Remote Sensing Center (NERSC), Thormøhlensgate 47, 5006 Bergen, Norway, Email: knut-frode.dagestad@nersc.no*

ABSTRACT

The sea area off the east coast of the Black Sea is an area where often pronounced local winds are encountered. The most prominent one is the Novorossiyskaya bora, which is a strong wind blowing from the coastal mountains onto the Black Sea, which can attain speeds of up to 40 ms^{-1}. But also katabatic winds and foehn winds are often encountered in this area. We have analyzed seven coastal wind events by using synthetic aperture radar (SAR) images acquired by the Advanced Synthetic Aperture Radar (ASAR) onboard the European Envisat satellite. The winds modify the sea surface roughness and thus they become visible on SAR images. Information on the spatial extent and the fine-scale structure of the coastal wind fields can be obtained from these images. In particular, SAR images can be used to study 1) wind jets, wakes, and atmospheric eddies generated by the interaction of winds with coastal topography, 2) boundaries between the local and ambient wind fields, and 3) atmospheric gravity waves (AGWs). Quantitative information on the near-surface wind field is derived from the SAR images by using the CMOD4 wind scatterometer model for converting radar backscatter values into wind speeds. It is argued that the east coast of the Black Sea is an ideal test area for validating meso-scale atmospheric models.

1. INTRODUCTION

The east coast of the Black Sea is an area where several pronounced local wind fields are encountered. Here the Black Sea is bordered by a coastal mountain range of variable height having several gaps and valleys through which airflow from the east can blow onto the Black Sea. In the southern section of the Black Sea, airflow passing from the east over Likhi Ridge can advance westward through a broad valley, called Kolkhida (or Kolkheti) Lowland or Rioni River Basin. The most famous local wind encountered at the east coast of the Black Sea is the Novorossiyskaya bora [1]. [2], [3], which can attain speeds of more than 40 ms^{-1} and can be quite hazardous, especially for coastal ship traffic and harbor operations.

In this paper we present seven synthetic aperture radar (SAR) images which were acquired by the Advanced Synthetic Aperture Radar (ASAR) onboard the European Envisat satellite (launched in 2002) over the eastern part of the Black Sea. From these images we derive the near-surface wind fields associated with these events.

In Section 3 we present three ASAR images showing sea surface signatures of bora winds, in Section 4 we present three ASAR images showing sea surface signatures of katabatic winds, and in Section 5 we present one ASAR image showing sea surface signatures of strong winds blowing from the Kolkhida lowland onto the Black Sea, which we interpret as being foehn winds. In order to strengthen our interpretation of the SAR images, we also use data from the scatterometer onboard the American Quikscat satellite [4], from the Moderate Resolution Imaging Spectroradiometer (MODIS) onboard the American Terra satellite (http://modis.gsfc.nasa.gov), and from local weather stations. Finally, in Section 6 we summarize the results.

2. RETRIEVAL OF NEAR-SURFACE WINDS FROM SAR IMAGES OF THE SEA SURFACE

Near-surface wind fields are obtained from SAR images via the measurement of the small-scale sea surface roughness. The stronger the wind, the rougher is the sea surface and thus the higher is the radar backscattering. SAR measures the backscattered radar power or normalized radar cross section (NRCS), which is a function of radar parameters and of wind speed and direction at the sea surface (or more precisely, of the wind stress) [5]. An empirical relationship, called CMOD4 model (C-band Scatterometer MODel, Version 4), has been developed to relate NRSC values measured by a C-band radar to the near-surface wind speed and direction. The SAR onboard the Envisat satellite operates at a frequency of 5.3 GHz and thus is a C-band band radar. The CMOD4 model was originally developed for the C-band wind scatterometer onboard the European Remote Sensing satellites ERS-1 and ERS-2 [6], but now it is also widely applied to the C-band ASAR onboard the Envisat satellite.

Since the NRCS values depend on the wind speed and direction, but SAR measures only one NRCS value per resolution cell, one has to get wind direction from other sources than from NRCS measurements for retrieving two-dimensional near-surface wind fields from SAR images of the sea surface. This information can be obtained from numerical atmospheric models or from the SAR image itself. Often linear features can be delineated on SAR images which are indicative for the direction of the near-surface wind. Such linear features include sea surface signatures of wind streaks and wind shadows behind islands and coastal mountains [7] - [11]. In this paper we take the wind direction from the NCEP model (Model of the National Centers for Environmental Prediction, USA). It provides global wind fields at a grid spacing of 0.5 degrees every three hours.

3. BORA WINDS

Bora winds are local down-slope winds, where cold air is pushed over a coastal mountain range due to a high pressure gradient or due to the passage of a cold front. They are encountered in mountainous coastal regions, where the mountain range is not too high (typically below 600 m) such that the adiabatic warming of the descending cold air is small. This is in contrast to foehn and Chinook winds where adiabatic warming is significant (see Section 5). Bora winds are best known from the east coast of the Adriatic Sea [12] - [20], but they are encountered also at the east coast of the Black

Sea. Since they occur mainly in the coastal areas near Novorossiysk (44.7ºN, 37.8ºE), they are also called Novorossiyskaya boras [1], [2]. When the wind is sufficiently strong and when it persists over a sufficiently long time (typically several days), then an oceanic cyclonic eddy is generated at the east coast of the Black Sea southeast of Tuapse (Russia).

3.1. The 15 December 2008 event

In Fig. 1 an Envisat ASAR image is depicted, which was acquired in the Wide Swath Mode (WSM) at HH polarization on 15 December 2008 at 19:10 UTC over the east coast of the Black Sea.

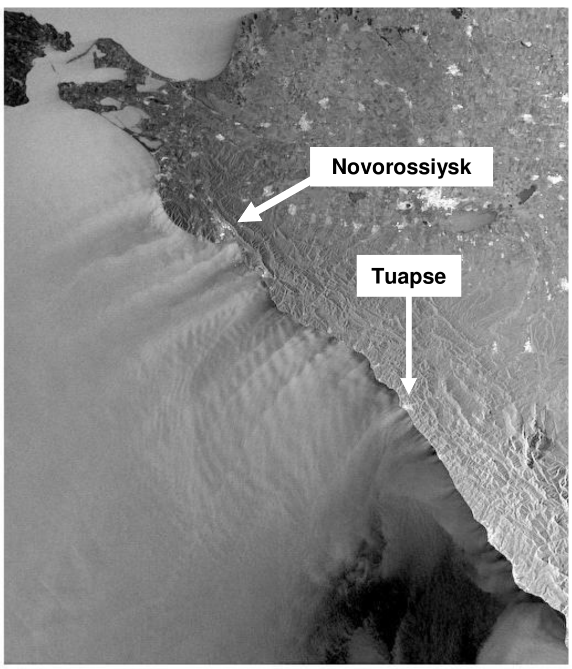

Fig.1. Envisat ASAR WSM image (HH polarization) acquired on 15 December 2008 at 19:10 UTC during a bora event over the east coast of the Black Sea. The imaged area is 400 km x 480 km. © ESA

Visible are sea surface signatures of strong wind jets and atmospheric gravity waves (AGWs). In Fig. 2 the near-surface wind field is depicted which was retrieved from this ASAR image by using the wind direction from the NCEP model. It shows that the wind jets have speeds of up to 20 ms^{-1} and that the dark area in the ASAR image is associated with a cyclonic atmospheric eddy. Note the low winds in the center of the eddy (see lower right-hand section of Fig.7).

The presence of AGWs touching the sea surface over a long distance requires that they are trapped in a wave guide [21]. The vertical walls of the wave guide are 1) the sea surface and 2) a strong inversion layer at a height of 826 m. The presence of an inversion layer at this height was inferred from radiosonde data acquired by the weather station at Tuapse on 15 December at 12:00 UTC (not reproduced here). The horizontal walls are the horizontal wind shear layers at the boundary between the high and low wind speed bands.

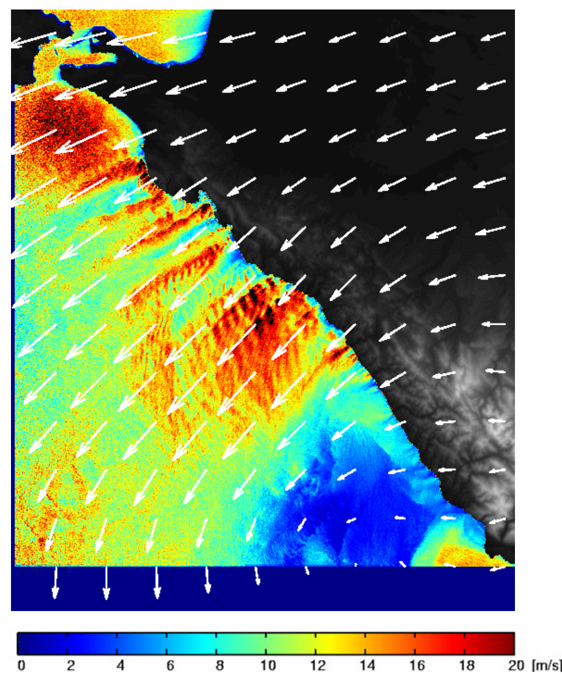

Fig. 2. Near-surface wind field retrieved from the ASAR image depicted in Fig. 1 by using the wind direction from the NCEP model showing wind jets with embedded atmospheric gravity waves.

3.2. The 5 February 2010 event

In Fig. 3 an Envisat ASAR image is depicted, which was acquired in the Wide Swath Mode (WSM) at VV polarization on 5 February 2010 at 07:45 UTC over the east coast of the Black Sea during another bora event, and in Fig. 4 is depicted the near-surface wind field retrieved from this ASAR image using the wind direction from the NCEP model at 09:00 UTC.

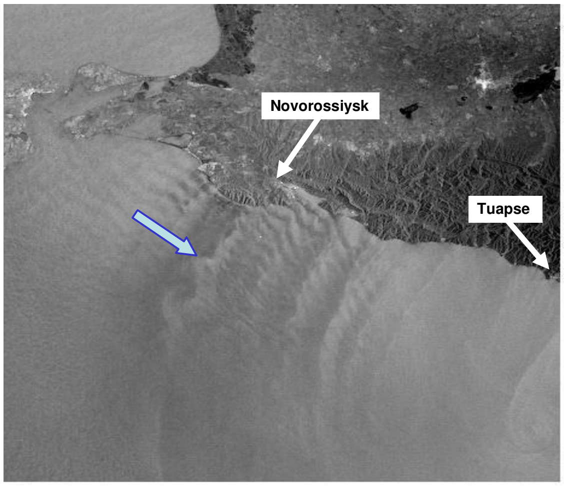

Figure 3. Envisat ASAR WSM image (VV polarization) acquired on 5 February 2010 at 07:45 UTC during a bora event over the east coast of the Black Sea. The imaged area is 240 km x 200 km. © ESA

It shows near Novorossiysk several high wind speed bands (areas of increased image brightness relative to the background) and between them low wind speed bands (areas of decreased image brightness). Note that the bands of increased image brightness result from airflow over low topography in the coastal mountain range. Noteworthy is the wavy structure of a boundary between a high wind speed band and a low wind speed band marked by an arrow. This wavy structure is very likely caused by Kelvin-Helmholtz instability. Embedded in the high wind bands (or wind jets) are AGWs propagating against the wind. In the earth reference system they are stationary. We infer from Fig. 4 that the wind speed variation caused the AGWs is approximately 4 ms^{-1} (varying between 12 and 16 ms^{-1}).

Fig. 5 shows a time series of the wind speed measured by the weather stations at Novorossiysk (dark blue) and at Tuapse (violet) starting on 2 February at 00:00 local time (UTC +3 h) and ending on 8 February 2010 at 21:00 local time. It shows that this bora lasted about two days. Note that at Tuapse (44.1ºN, 39.1ºE), the wind speed was quite low during the whole period. Here the airflow from the east was blocked by the high mountains. Thus a strong horizontal wind shear was generated over the sea giving rise to the formation of a cyclonic eddy over the southeastern section of the Black Sea. This cyclonic eddy is visible on the MODIS Terra color composite image depicted in Fig. 6, which was acquired at 08:05 UTC, i. e., only 20 minutes after the

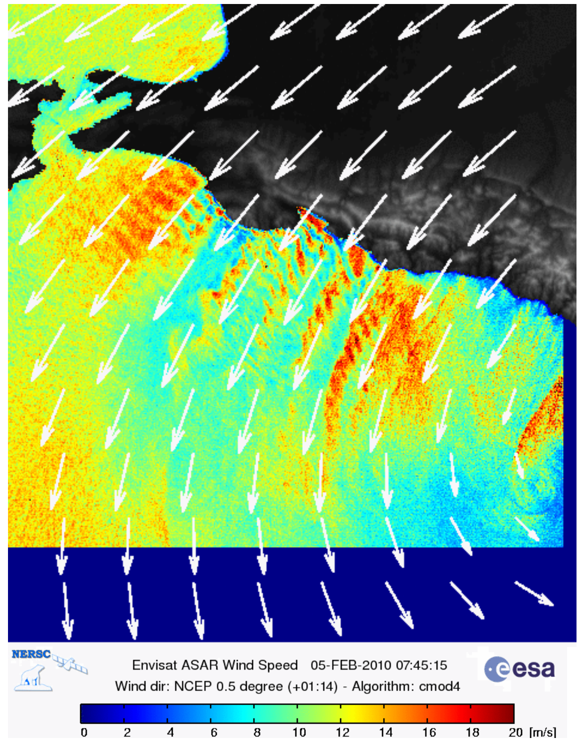

Figure 4. Near-surface wind field retrieved from the ASAR image depicted in Fig. 3 by using the wind direction from the NCEP mode. It shows wind jets with embedded atmospheric gravity waves.

ASAR image. It shows in the cloud pattern a cyclonic eddy and also AGWs near Novorossiysk.

.

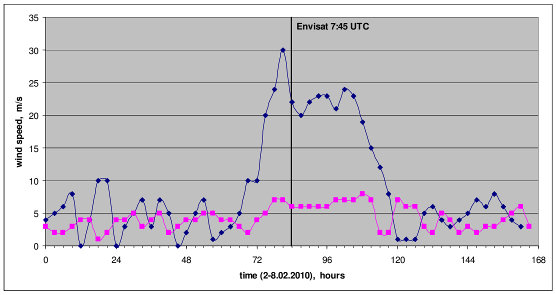

Figure 5. Wind speed measured at the Novorossiysk (dark blue) and Tuapse (violet) weather stations from 00:00 local time (UTC +3 h) on 2 February to 21:00 local time on 8 February 2010. The time of the ASAR data on 5 February at 07:45 UTC is marked by the vertical dark line.

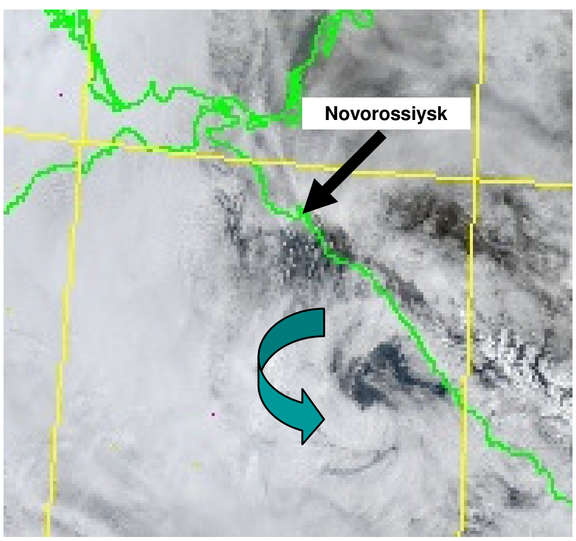

Figure 6. MODIS Terra color composite image of the east coast of the Black Sea around Novorossiysk acquired on 5 February 2010 at 08:05 UTC showing in the cloud pattern a cyclonic eddy (marked by the inserted arrow) and atmospheric gravity waves near Novorossiysk. © NASA GSFC

3.3. The 2 November 2009 event

In Fig. 7 an Envisat ASAR image is depicted, which was acquired in the Wide Swath Mode (WSM) at VV polarization on 2 November 2009 at 07:31 UTC over

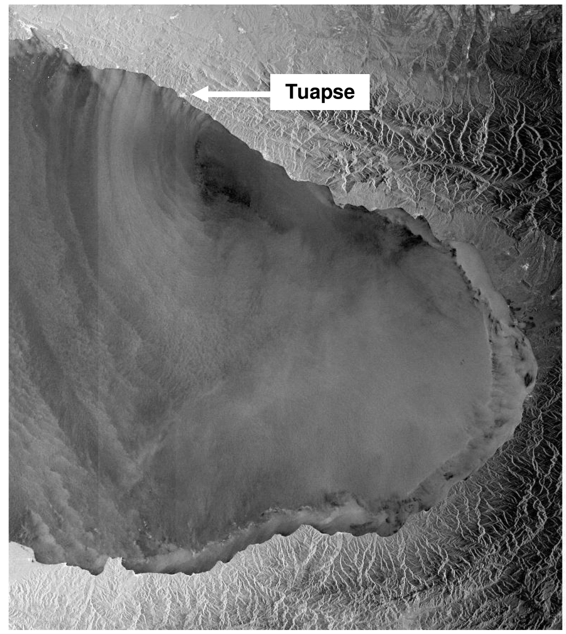

Figure 7. Envisat ASAR WSM image (VV polarization) acquired on 02 November 2009 at 07:31 UTC (10:31 local time) over the eastern section of the Black Sea showing in the northern section a wind jet and along the southern and souteastern shore a distinct roughness band. The imaged area is 400 km x 470 km. © ESA

the eastern section of the Black Sea and in Fig. 8 the near-surface wind field is depicted which was retrieved from this ASAR image using the wind direction from the NCEP model at 09:00 UTC. It shows in the northern section a strong wind jet with speeds around 16 ms^{-1} emanating from the coast.

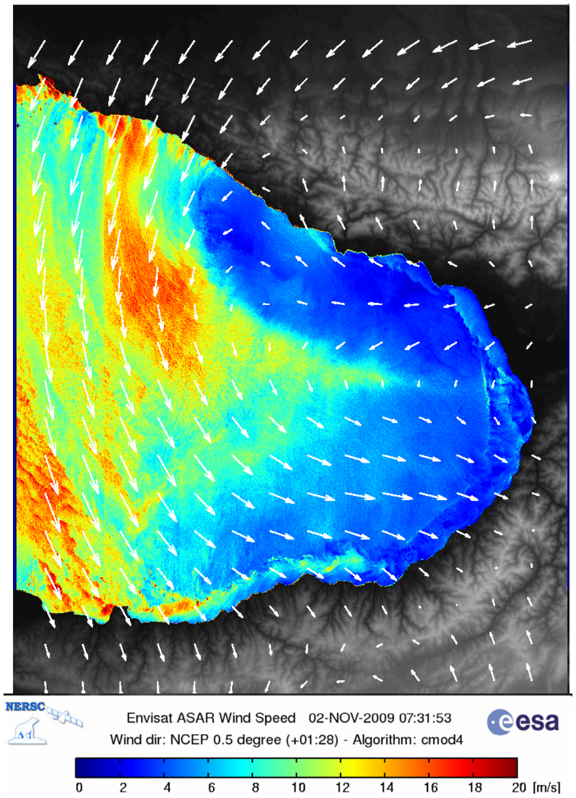

Figure 8. Near-surface wind field retrieved from the ASAR image depicted in Fig. 7 by using the wind direction from the NCEP model showing in the northern section a strong wind jet having a speed up to 17 ms^{-1} emanating from the coast. Due to wind shadowing by the high mountains to the south, the jet is deflected in a southward direction forming a cyclonic eddy

Due to wind shadowing by the high mountains south of Tuapse, the wind jet is deflected into a southward direction giving rise to the formation of a cyclonic eddy. The cyclonic wind pattern is also visible in the map of the near-surface wind field derived from Quikscat data acquired 3 hours and 7 minutes earlier (at 04:24 UTC), see Fig. 9. However, Quikscat measured a wind speed of only 13 ms^{-1} north of Tuapse. This is due to the fact that Quikscat has a much coarser spatial resolution (25 km) than ASAR and cannot resolve small-scale high wind speed areas.

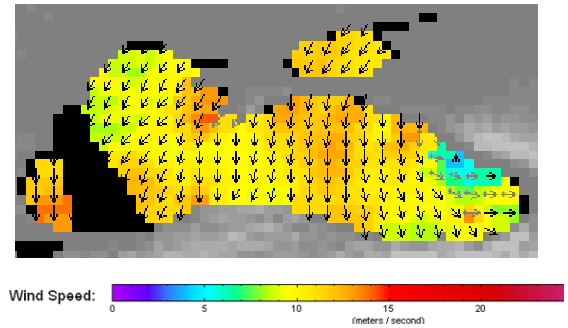

Figure 9. Near-surface wind field derived from Quikscat data acquired over the Black Sea on 02 November 2009 at 04:24 UTC showing at the east coast the deflection of the northerly wind eastwards. © Remote Sensing Systems

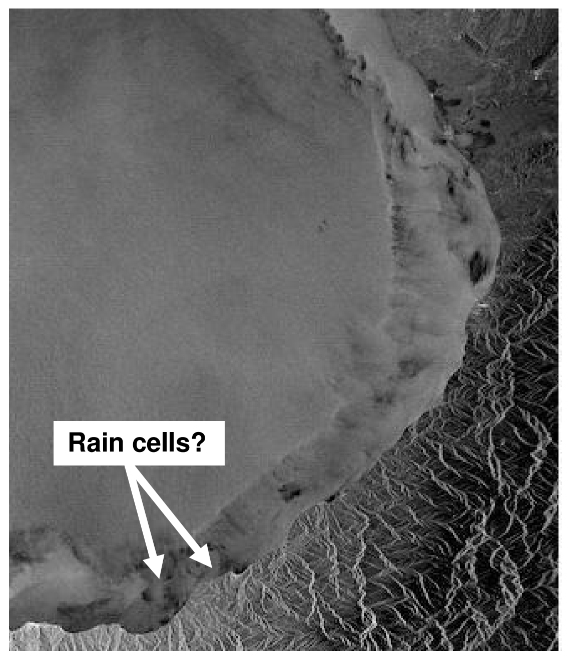

Figure 10. Zoom on the eastern section of the ASAR image depicted in Fig. 7 showing a coast-parallel roughness band.

A peculiar feature visible on the ASAR image depicted in Fig. 7 is an almost coast-parallel roughness band at the south and southeast coasts of the Black Sea, which is shown in more detail in Fig. 10. It has a sharp boundary with the ambient wind. The roughness band is quite inhomogeneous which we attribute to the unstable air-sea interface due to the fact that the air is much cooler than the water. It seems that rain cells are embedded in the coastal band. There seems to be no katabatic wind present blowing from the mountains onto the sea, see Section 4. Thus the frontal line seems not to be generated by the interaction of katabatic winds with the onshore synoptic-scale wind. Arguments in favor of this interpretation are:

1) The ASAR image was taken at 10:31 local time, i.e., at a time when no katabatic winds should be present.

2) The MODIS image shows cloud coverage at the coast.

3) The linear features visible in the coast-parallel roughness band seem to be outcrops of the synoptic-scale wind pattern and directed towards the coast.

It could be that the frontal line is generated by recirculation of on-shore wind interacting with the mountain range as described in [11]. However, this would not explain why the frontal line is also present at the coast line next to the Kolkhida lowland (Rioni River Basin), see Subsection 5.1. Here are no mountains which block the onshore airflow of the synoptic-scale wind Maybe that here the onshore airflow is blocked by a westward airflow from the Kolkhida lowland.

4. KATABATIC WINDS

Katabatic winds are cold winds blowing in the evening, at night, and early in the morning down a sloping terrain onto the sea. They are generated because air near the surface cools faster over the land than over the sea. This results in a down-hill flow of the cold air, called gravity flow. A prerequisite for the generation of katabatic winds is that the air can cool off significantly fast during the evening and night hours, which is usually the case when the cooling process is not impeded by (low-level) clouds, i.e., when the sky is cloud-free. The down-hill flow is funneled through coastal valleys and thus the sea surface signatures of katabatic winds look like "tongues" attached to coastal valleys [22].

4.1. The 16 January 2009 event

In Fig. 11 an Envisat ASAR image is depicted, which was acquired in the Image Mode (IMM) at VV polarization on 16 January 2009 at 19:02 UTC over the eastern section of the Black Sea and in Fig. 12 the near-surface wind field is depicted which was retrieved from

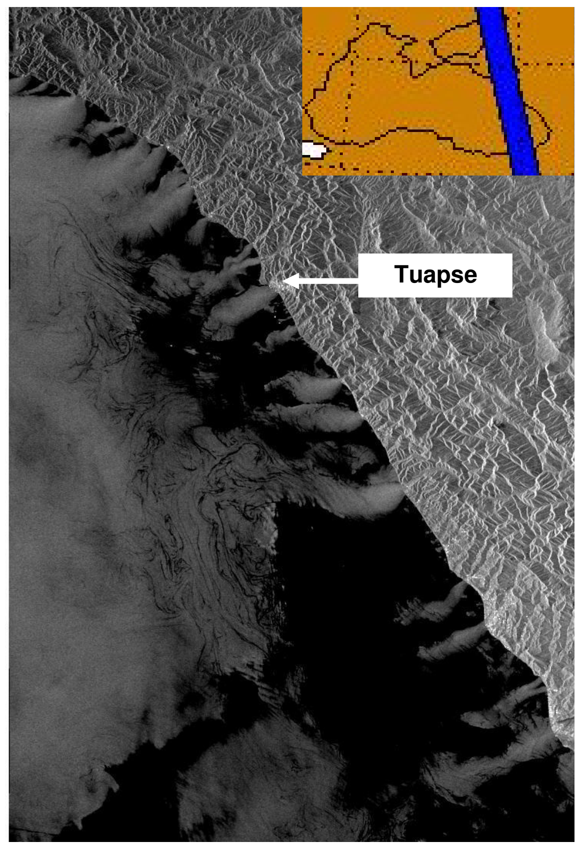

Figure 11. Envisat ASAR IMM image (VV polarization) acquired on16 January 2009 at 19:02 UTC over the eastern section of the Black Sea (see inserted map) showing sea surface signatures of katabatic winds emanating from coastal valleys. The imaged area is 100 km x 160 km. © ESA

this ASAR image using the wind direction from the NCEP model at 18:00 UTC.

This image shows typical sea surface signatures of katabatic winds emanating from several small coastal valleys. The ambient wind must have had speeds below the threshold for surface ripple generation (around 2 ms^{-1}). Thus the katabatic wind having speeds between 4 and 6 ms^{-1} could propagate offshore with little attenuation. The weak ambient wind was blowing from a southeasterly direction which bended the airflow of the katabatic wind slightly towards northwest.

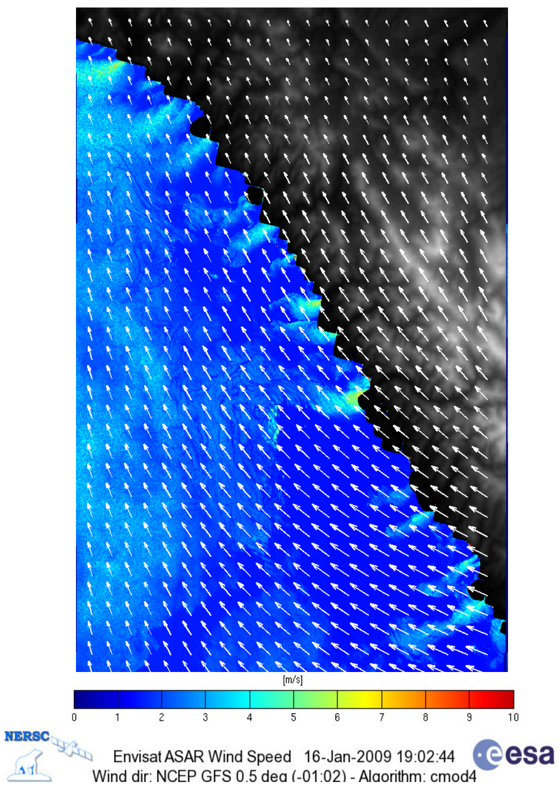

Figure 12. Near-surface wind field retrieved from the ASAR image depicted in Fig. 11 by using the wind direction from the NCEP model showing katabatic wind tongues in the near surface wind pattern.

In Fig. 13 a MODIS Terra color composite image of the eastern section of the Black Sea is depicted which was acquired on 16 January 2009 during daytime (12:00 local time = 09:00 UTC). It shows a cloud-free zone along the east coast of the Black Sea allowing the air over the mountains to cool off sufficiently fast during

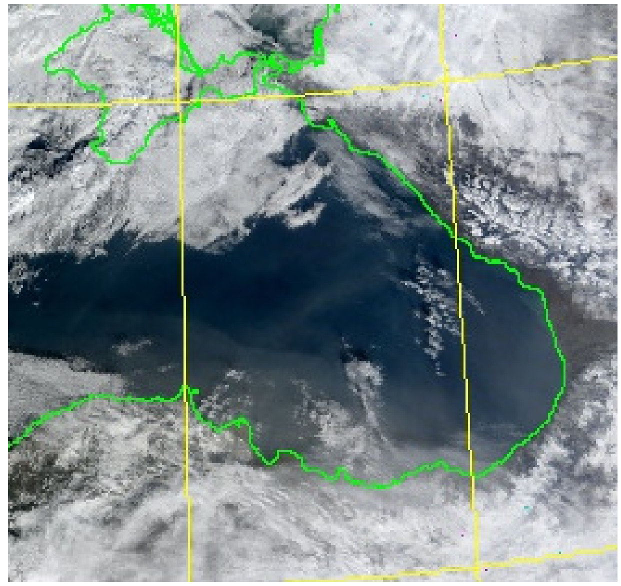

Figure 13. MODIS Terra color composite image of the eastern section of the Black Sea acquired on 16 January 2009 at 0900 UTC showing a cloud-free zone along the east coast of the Black Sea. © NASA GSFC

evening and night hours to generate downhill gravity flow. Note that the ASAR image was acquired at 22:02 local time, i.e., at a time when one expects katabatic winds.

4.2. The 30 April 2008 event

In Fig. 14 an Envisat ASAR image is depicted, which was acquired in the Alternating Polarization Mode (APM) at VV polarization on 30 April 2008 at 19:07 UTC over the eastern section of the Black Sea and in Fig. 15 the near-surface wind field is depicted which was retrieved from this ASAR image using the wind direction from the NCEP model at 18:00 UTC. Visible are again "wind tongues" emanating from coastal valleys having speeds around 8 ms^{-1}. However, during

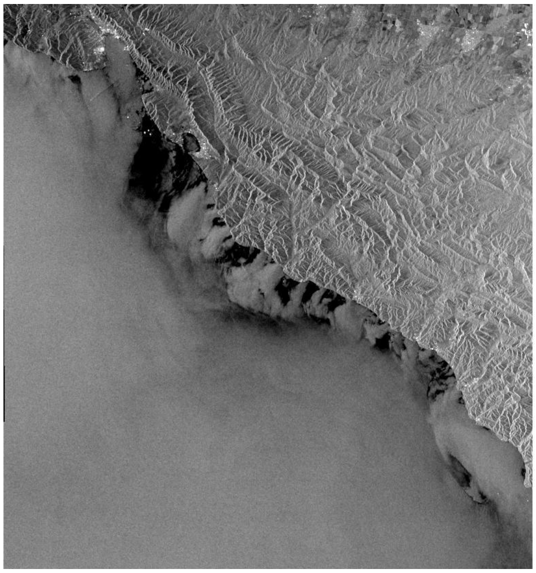

Fig. 14. Envisat ASAR APM image (VV polarization) acquired on 30 April 2008 at 19:07 UTC over the eastern section of the Black showing sea surface signatures of katabatic winds emanating from coastal valleys. The imaged area is 100 km x 160 km. © ESA

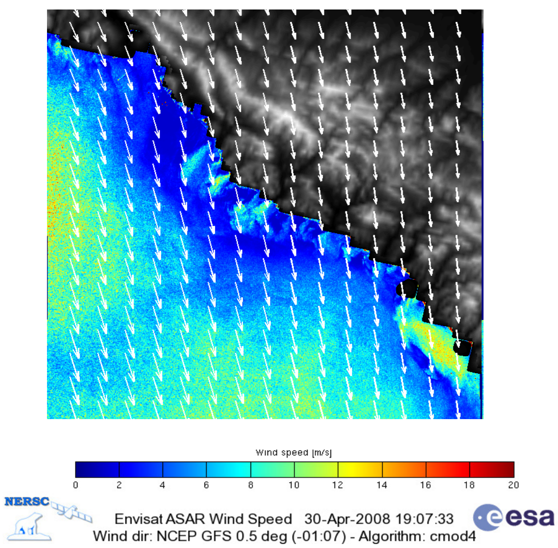

Figure 15. Near-surface wind field retrieved from the ASAR image depicted in Fig.14 by using the wind direction from the NCEP model showing katabatic wind tongues in the near surface wind pattern.

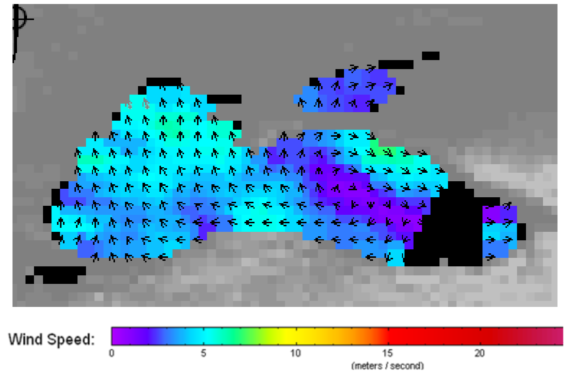

Fig. 16. Near-surface wind field derived from Quikscat data acquired over the Black Sea on 30 April 2008 at 16:54 UTC showing weak northwesterly winds at the northeast coast of the Black Sea,

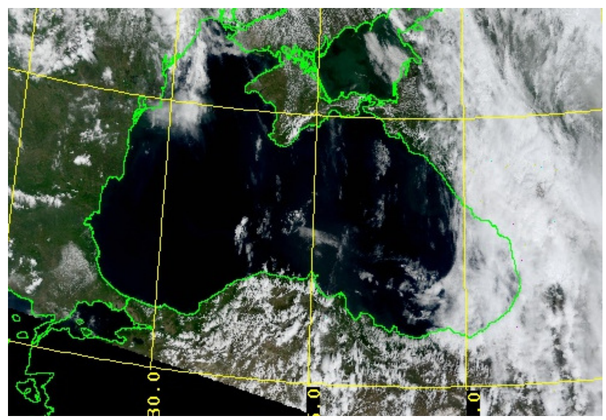

Fig. 17. MODIS Terra color composite image of the Black Sea acquired on 30 April 2008 at 08:40 UTC showing a cloud-free zone along the northeast coast of the Black Sea.

this event the ambient wind was slightly higher and interacted more strongly with the airflow of the katabatic wind. While the NCEP model predicted a northerly direction of the ambient wind (1 hour and 7 minutes before the ASAR data acquisition), Quikscat measured a north westerly direction with a speed between 6 and 8 ms^{-1} (Fig. 16). Thus the katabatic wind encountered an ambient wind which had a component in opposite direction. This caused a deformation of the katabatic wind pattern. Also on this day there were no clouds present along the east coast of the Black Sea (Fig. 17) and thus the air could cool off during the night over the mountains.

4.3. The 25 December 2007 event

In Fig. 18 an Envisat ASAR image is depicted, which was acquired in the Image Mode (IMM) at VV

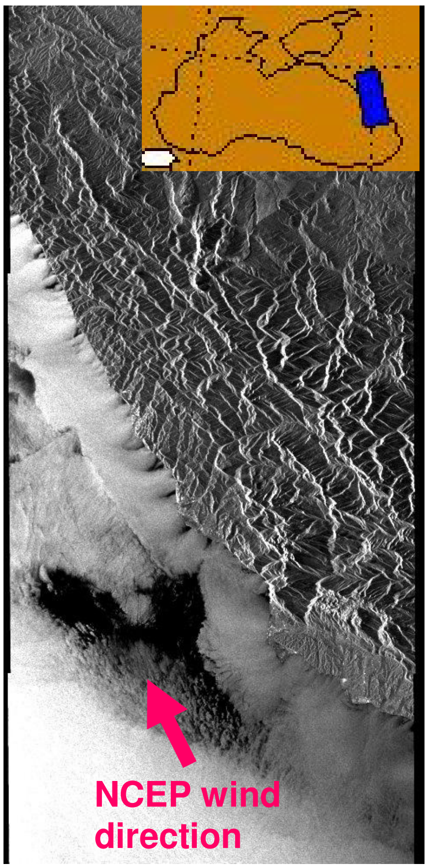

Figure 18. Envisat ASAR IMM image (VV polarization) acquired in the IS1-swath (incidence angles:15-19 degrees) on 25 December 2007 at 18:58 UTC over the eastern section of the Black Sea (see inserted map) showing sea surface signatures of katabatic winds emanating from coastal valleys The imaged area is 100 km x 230 km.

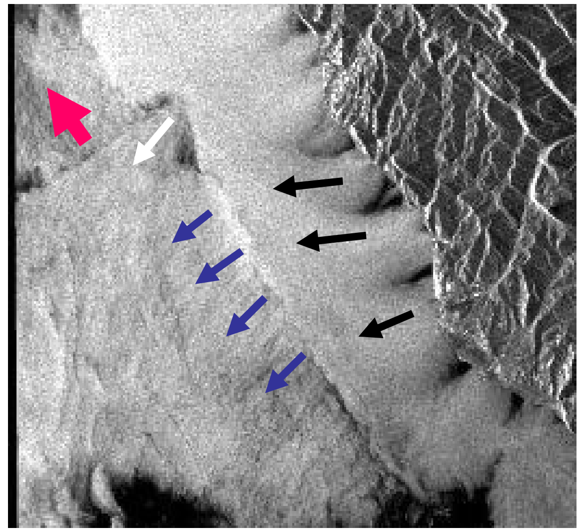

Figure 19. Zoom on the central section of the ASAR image depicted in Fig. 18. The arrows inserted in the image show the direction of linear features in the roughness pattern which are indicative for the wind direction.

polarization on 25 December 2007 at 18:58 UTC over the eastern section of the Black Sea.

Although the roughness pattern associated with the katabatic wind event looks very bright, the wind speed was only 3 to 4 ms^{-1} , which is due to the fact that this image was acquired in the IS1 swath where the incidence angle is very steep (15^0-19^0) and thus the NRCS is very large [5]. In this incidence angle range the algorithm for retrieving near-surface wind fields from SAR images is quite inaccurate and therefore we have refrained from plotting the wind field for this event. The NCEP model predicted at 18:00 UTC a coast-parallel wind from southeast.

However, the roughness pattern visible on the ASAR image (Fig. 18) yields quite unexpected details of the structure of the wind field. A zoom on the central section of this image is depicted in Fig. 19. Several linear features can be delineated in the roughness pattern which we interpret as being indicative for the direction of the near-surface wind field, which are marked by arrows. The black arrows indicate the direction of the katabatic wind and the red arrow the direction of the ambient wind, which is in agreement with the direction predicted by the NCEP model, see Fig.18. The white arrow seems to indicate a divergent airflow and the blue arrows seem to indicate a weak off-shore airflow beyond the primary airflow of the katabatic wind. So far, we have no explanation for the airflows marked by the white and blue arrows.

5. FOEHN WINDS

Foehn winds are warm winds encountered on the lee side of mountain ridges due to the downward movement of airflow. They are associated with an increase in air temperature, reduction of relative humidity and dispersal of the lower layer clouds. Foehn are common wind events on the north side of the Alps (e.g., in Munich, Germany).

5.1. The 11 January 2010 event

In Fig. 20 an Envisat ASAR image is depicted, which was acquired in the Image Mode (IMM) at VV polarization on 11 January 2010 at 07:31 UTC over the south eastern section of the Black Sea and in Fig. 21 the near-surface wind field which was retrieved from this ASAR image by using the wind direction from the NCEP model at 09:00 UTC. Fig. 20 shows in the central section a broad roughness band caused by wind blowing through the Kolkhida lowland (Rioni River Basin) in Georgia onto the sea. The roughness band is quite inhomogeneous due to the interaction of the easterly wind with uneven topography in the Kolkhida lowland. Furthermore, Fig. 20 shows in the lower section sea surface signatures of strong winds blowing through gaps in the coastal mountains in southern Georgia and northern Turkey. In both sections sea surface signatures of AGWs are visible.

Figure 20. Envisat ASAR IMM image (VV polarization) acquired on 11 January 2010 at 07:31 UTC over the south eastern section of the Black Sea (see inserted map) showing sea surface signatures of foehn winds blowing through the Kolkhida lowland (Rioni River Basin) in Georgia and though gaps in the coastal mountain range in northern Turkey. Embedded are atmospheric gravity waves. The imaged area is 100 km x 220 km. © ESA

We hypothesise that the roughness band in the central section is the sea surface signature of foehn winds emanating from the Kolkhida lowland and generated by airflow over the Likhi ridge. As stated in [23], the Kolkhida lowland is a region having all conditions for the development of foehn winds due to its topography. The Kolkhida lowland is bordered by high mountains (the Greater and Lesser Caucasian mountain ranges) and has the form of a triangle which opens to the sea (Fig. 22). The eastern corner of this triangle is located at Likhi ridge which connects the Greater Caucasus with the Lesser Caucasus ranges. The Likhi ridge has heights between 1926 m and 946 m (Surami Pass) over which air from the east can flow into the Kolkhida lowland. According to Gunia et al. [23], this usually occurs when a Low is located over the Black Sea and a High over Middle Asia. Indeed, the weather map of 11 January 2010 at 06:00 UTC (Fig. 23) shows that a High was situated southeast of the Black Sea and a Low over its northwest coast pushing air over the Likhi ridge into the Kolkhida lowland. Meteorological data acquired by the weather station at Kutaisi, which is located approximately mid-way between the Likhi ridge and the Black Sea (see Fig. 22), are listed in Table 1. They show that during the ASAR data take the air temperature was much higher and the humidity much lower than at the same time two days before and one day later. This suggests that during the time of the ASAR data acquisition foehn winds were blowing through the Kolkhida lowland. This interpretation is further supported by a cloud image (Fig. 24), which was acquired by the MODIS sensor onboard the Terra satellite on 11 Jan 2010 at 08:10 UTC, i.e., 39 minutes after the ASAR data acquisition. It shows near the Likhi ridge a cloud-free region, which is characteristic for foehn events.

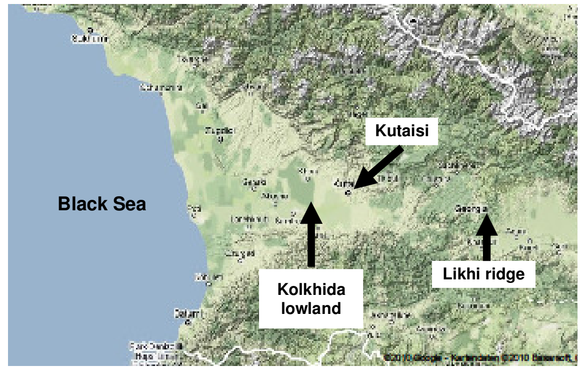

Figure 22. Topography of the Kolkhida lowland (Rioni River Basin . © Google maps

Table 1: Meteorological data measured at Kutaisi

	2 days before, same time	Time of ASAR data acquisition	1 day after, same time
Wind speed	10 m/s	10 m/s	
Air temperature	13^0 C	19^0 C	8^0 C
Relative humidity	32%	19%	60%

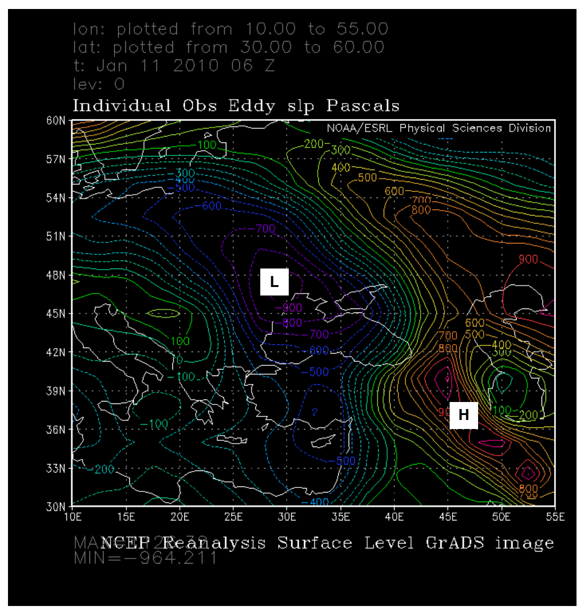

Figure 23. Surface eather map of 11 January 2010 at 06:00 UTC showing a high pressure region southeast and a low pressure region northwest of the Black Sea.

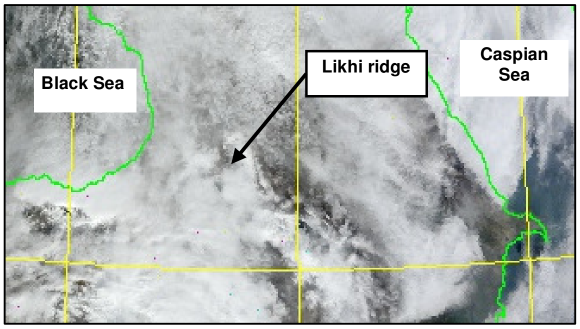

Figure 24. MODIS Terra color composite image of the Black Sea acquired on 11 January 2010 at 08:10 UTC showing a cloud-free zone at the Likhi ridge.

6. SUMMARY

The east coast of the Black Sea is an area of complex coastal topography which gives rise to several distinct coastal winds. In the northern section, the coastal mountains between Novorossiysk and Tuapse have a height around 600 m, but further south they have heights exceeding 1500 m. Between Novorossiysk and Tuapse often very high winds are encountered, which are called Novorossiyskaya boras. They can attain speeds above 40 ms^{-1} and often cause large damage at the coast, including ship sinking. This wind is similar to the bora wind encountered at the east coast of the Adriatic Sea.

The high mountains south of Tuapse block the airflow from the east. This gives rise to a very pronounced coastal wind pattern in the southeastern section of the Black Sea. The airflow from the east experiences a torque and thus is deflected into a southward direction. This initializes a cyclonic atmospheric eddy (see Figs. 1, 6, and 7). During the 2 November 2009 event (Fig.7) the northerly synoptic-scale wind interacted strongly with the mountain range at the southern and southeastern coast of the Black Sea generating a distinct coast-parallel roughness band. The mechanism which causes this roughness band separated by the ambient wind field by a frontal line is not yet fully understood.

Furthermore, the coastal mountain range south of Tuapse has many small valleys opening to the sea through which cold air can flow downhill late in the evening and at night. which gives rise to “tongue-like” wind fields attached to the coastal valleys. These winds are called katabatic winds and can vary in distance and shape depending on their strength and the strength and direction of the ambient wind as shown in three ASAR images (see Figs. 11, 14, and 18).

At the southeast coast of the Black Sea a broad valley, through which the Rioni river is flowing, opens to the sea. Through this valley often foehn winds are blowing which are generated by airflow from the east/southeast passing the Likhi ridge. The highest height of this ridge is 1926 m..

By using the CMOD4 wind scatterometer model and by taking the wind direction from the NCEP model, we have been able to derive near-surface wind fields from the SAR images. However, not in all cases this method yielded satisfactory results. In some cases the wind retrieval method used in this paper needs to be supplemented by another wind retrieval method which derives wind directions from linear features visible on SAR images.

Some of the SAR images presented in this paper have revealed fine-scale features of coastal wind fields (Fig. 7 and 19) for which we have no satisfactory theoretical explanation yet. Thus these SAR images should motivate modelers to simulate the wind fields with the aim to explain the physical mechanisms giving rise to these fine-scale features in the coastal wind fields features. We consider the east coast of the Black Sea to be an ideal area to validate meso-scale atmospheric models.

ACKNOWLEDGEMENT

We thank ESA for providing the Envisat ASAR images within the frameworks of the ESA Envisat AO project C1P.3424.

6. REFERENCES

1. Burman, E. A. (1969), Local Winds, Leningrad, *Gidrometeoizdat,* 342 p. *(*in Russian*).*
2. Gusev, A. M. (Ed.) (1959). Novorossiyskaya Bora, *Proceedings of Marine Hydrophysical Institute AN* USSR, **14**. 157 *(*in Russian*).*
3. Alpers, W., Ivanov, A., & Horstmann, J. (2009), Observations of bora events over the Adriatic Sea and Black Sea by spaceborne synthetic aperture radar, *Mon. Wea. Rev*., **137**(**3**), 1154-1165, doi: 10.1175/2008MWR2563.1.
4. Liu, W. T., Tang, W., & Polito, P. S. (1998), NASA scatterometer provides global ocean-surface wind fields with more structures than numerical weather prediction, *Geophys. Res. Lett*., **25**, 761-764.
5. Valenzuela, G. R. (1978), Theories for the interaction of electromagnetic and oceanic waves: A review, Bound.-Layer Meteor., **13**, 61-85.
6. Stoffelen, A. & Anderson, D. (1997), Scatterometer data interpretation: Estimation and validation of the transfer function CMOD4, *J. Geophys. Res*., **102**, 5767-5780.
7. Horstmann, J., Koch, W., Lehner, S., & Rosenthal, W. (1998), Ocean wind field and their variability derived from SAR, *Earth Observ. Quart*., **59**, 8-12.
8. Monaldo, F., Kerbaol, V., & the SAR Wind Team (2003), The SAR measurement of ocean surface winds: An overview, *Proc. 2nd Workshop on Coastal and Marine Applications of SAR*, 8-12 September 2003, Svalbard, Norway.
9. Monaldo, F. M., Thompson, D. R., Beal, R. et al. (2001), Comparison of SAR derived wind speed with model predictions and ocean buoy measurements, *IEEE Trans. Geosci. Rem. Sens*., **39**, 2587-2600.
10. Horstmann, J. & Koch, W. (2005), Comparison of SAR wind field retrieval algorithms to a numerical model utilizing Envisat ASAR data*, IEEE J. Ocean Eng*., **30**, 508-515. doi 10.1109/JOE.2005.857514.
11. Alpers, W., Chen, J. P., Pi, Ch.-J., & Lin, I-I (2010), On the origin of atmospheric frontal lines off the east coast of Taiwan observed on space-borne synthetic aperture radar images, *Mon. Wea. Rev*., **138**, 475-496,doi:10.1175/2009MWR2987.1.
12. Prettner, J. (1866), Die Bora und der Tauernwind, *Zeitsch. der oesterr. Gesellsch. f. Met*., **1**(**14**), 210-214 and **1**(**15**), 225 -230.
13. Yoshino, M. M. (Ed.) (1976), Local wind Bora, *Univ. of Tokyo Press,* Tokyo.
14. Smith, R. B. (1987), Aerial observation of the Yugoslavian bora, *J. Atm. Sci*., **44**, 269 -297.
15. Klemp, J. B. & Durran, D. R. (1987), Numerical modeling of bora winds, *Meteorol. Atmos. Phys.*, **36**. 215-227.
16. Petkovšek, Z. (1987), Main bora gusts – a model explanation, *Geofisika,* **4**. 41 -50.
17. Dorman, C. E., Carniel, S., Cavaleri, L. et al. (2007), February 2003 marine atmospheric conditions and the bora over the northern Adriatic, *J. Geophys. Res.*, **112(C3).** doi: 10.1029/2005JC003134.
18. Gohm, A., Mayr, G. J. (2005), Numerical and observational case-study of a deep Adriatic bora, *Q. J. R. Meteorol. Soc*., **131**, 1363-1392.
19. Cushman-Roisin, B. & Korotenko, K.A. (2007). Mesoscale-resolving simulations of summer and winter bora events in the Adriatic Sea, *J. Geophys. Res.* **112(C3).** doi10.1029/2006JC003516.

20. Signell, R. P., Chiggiato, J., Horstmann, J., Doyle, J. D., Pullen, J., & Askari, F. (2010), High-resolution mapping of Bora winds in the northern Adriatic Sea using synthetic aperture radar, *J. Geophys. Res.*, **115**, C04020, doi:10.1029/2009JC005524.
21. Cheng, C. M. & Alpers, W. (2010), Investigation of trapped atmospheric gravity waves over the South China Sea using Envisat synthetic aperture radar images, *Int. J. Remote Sensing*, in press.
22. Alpers, W., Pahl, U., & Gross, G. (1998), Katabatic wind fields in coastal areas studied by ERS-1 synthetic aperture radar imagery and numerical modeling, *J. Geophys. Res*., **103**, 7875 -7886.
23. Gunia, G., Tskvitinidze, Z., Kholmatjanov, B., & Fatkhullaeva, Z. (2008), Influence of foehn phenomena on the processes of atmospheric air pollution*, Bulletin of the Georgian National Academy of Sciences*, **2** (**3**), 65- 69.